Supporting Information

Global Gridded Air-sea Oxygen Flux Inferred from a Machine Learning-based Dissolved Oxygen Product

Yuming Jin et al.

Correspondence: Yuming Jin (yumingjin@ucar.edu)

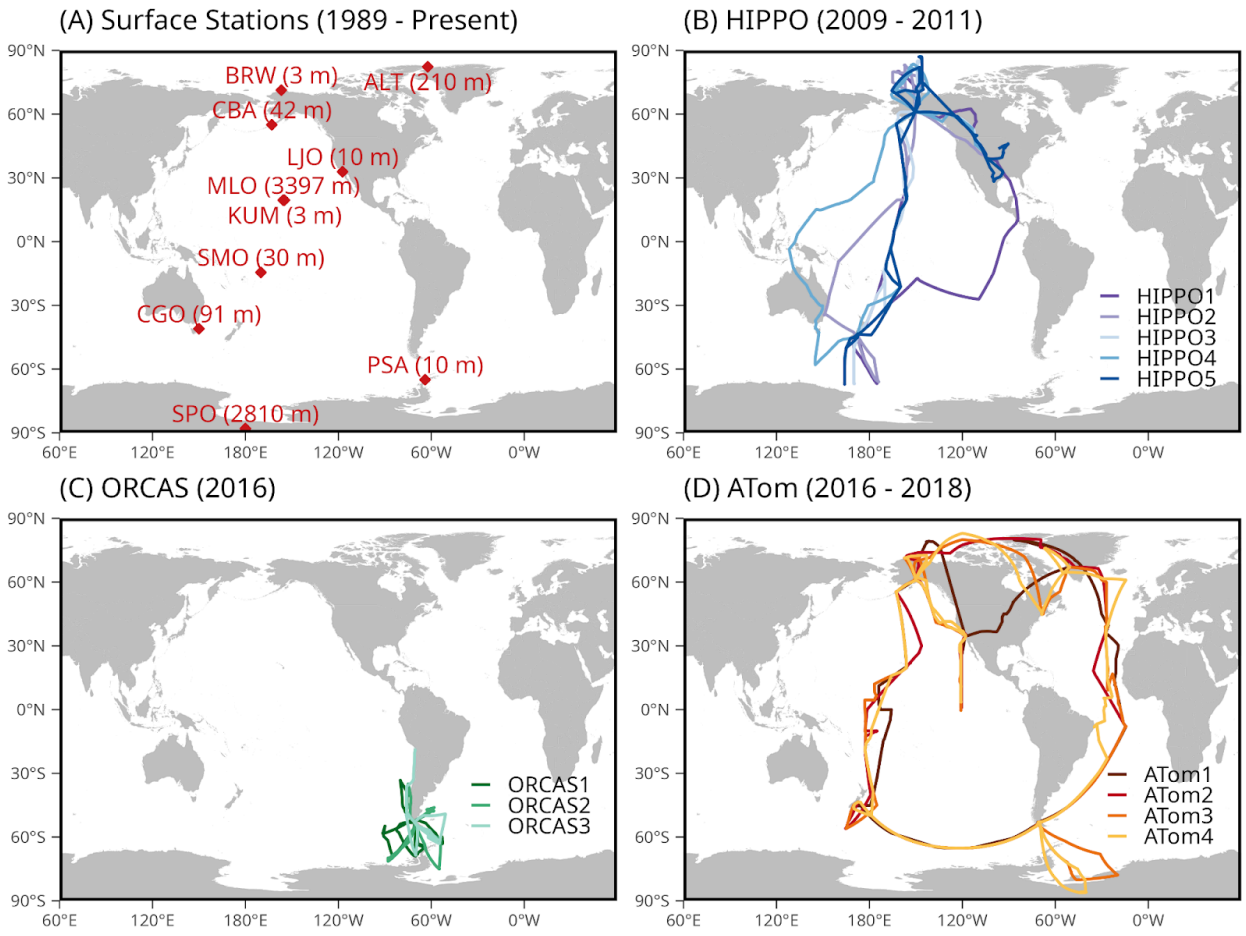

Fig. S1: Horizontal distribution of station and airborne measurements that provide atmospheric O_2 measurements used to evaluate the air-sea O_2 flux product. (A) Scripps O_2 program stations with station codes and inlet elevation in meters above sea level. (B) - (D) HIPPO, ORCAS, and ATom airborne campaign horizontal flight tracks.

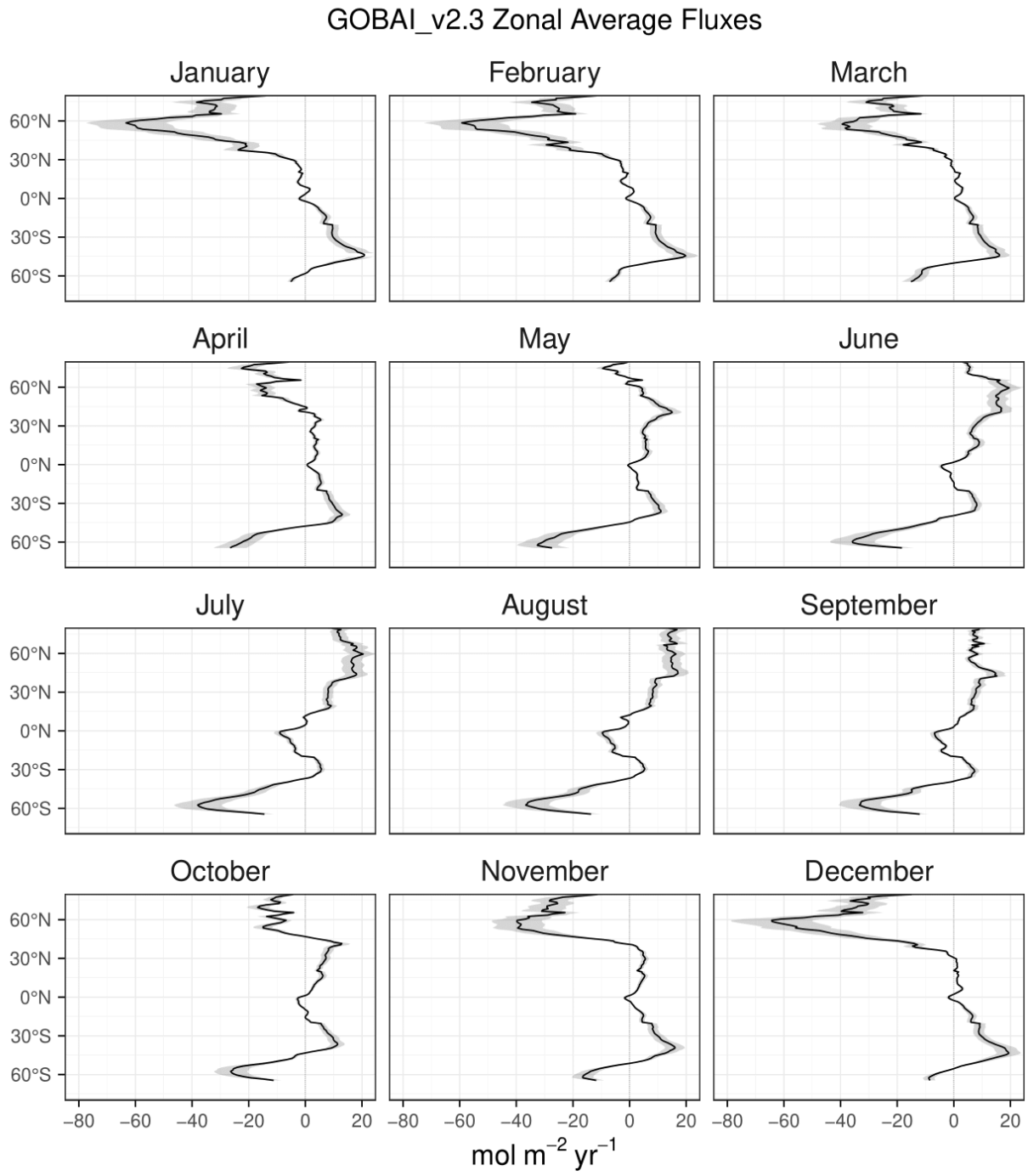

Fig. S2: Ensemble mean zonal mean flux (black lines) and 1σ uncertainty (gray shades) of each month, averaged from 2004 to 2024.

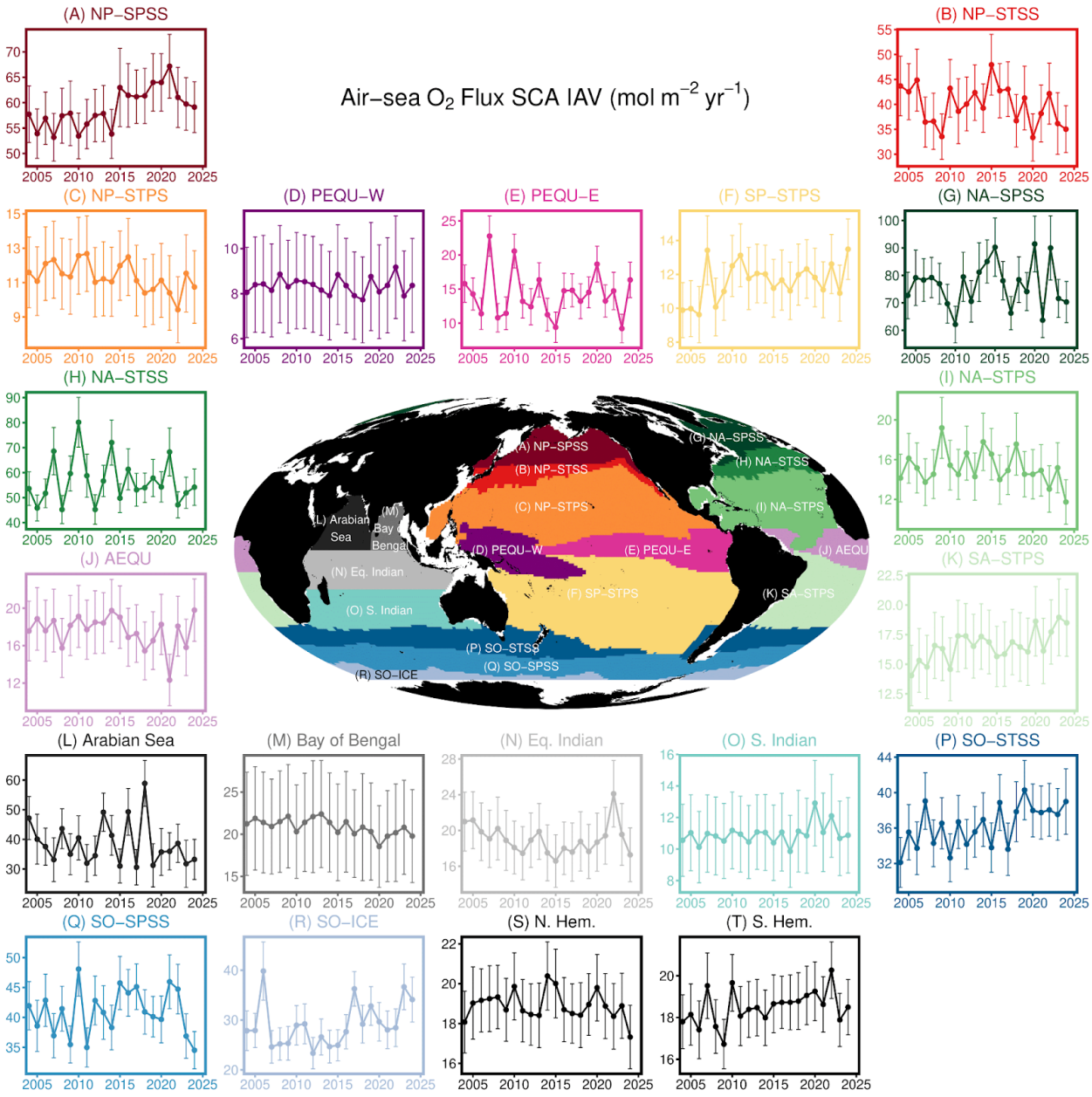

Fig. S3: Interannual variability of air-sea O_2 flux SCA. SCA is calculated by first fitting a 2-harmonic function to the monthly flux climatology of each region and each individual year, then taking the difference between the seasonal maximum and minimum. Error bars represent uncertainty calculated as standard deviation of all ensemble members. Panels are organized in the same order and colors as in Fig. 2. Panel titles and colors correspond to the region names and colors shown in the center map. Y-axis ranges vary across panels to optimize visualization of seasonal flux amplitude for each region.

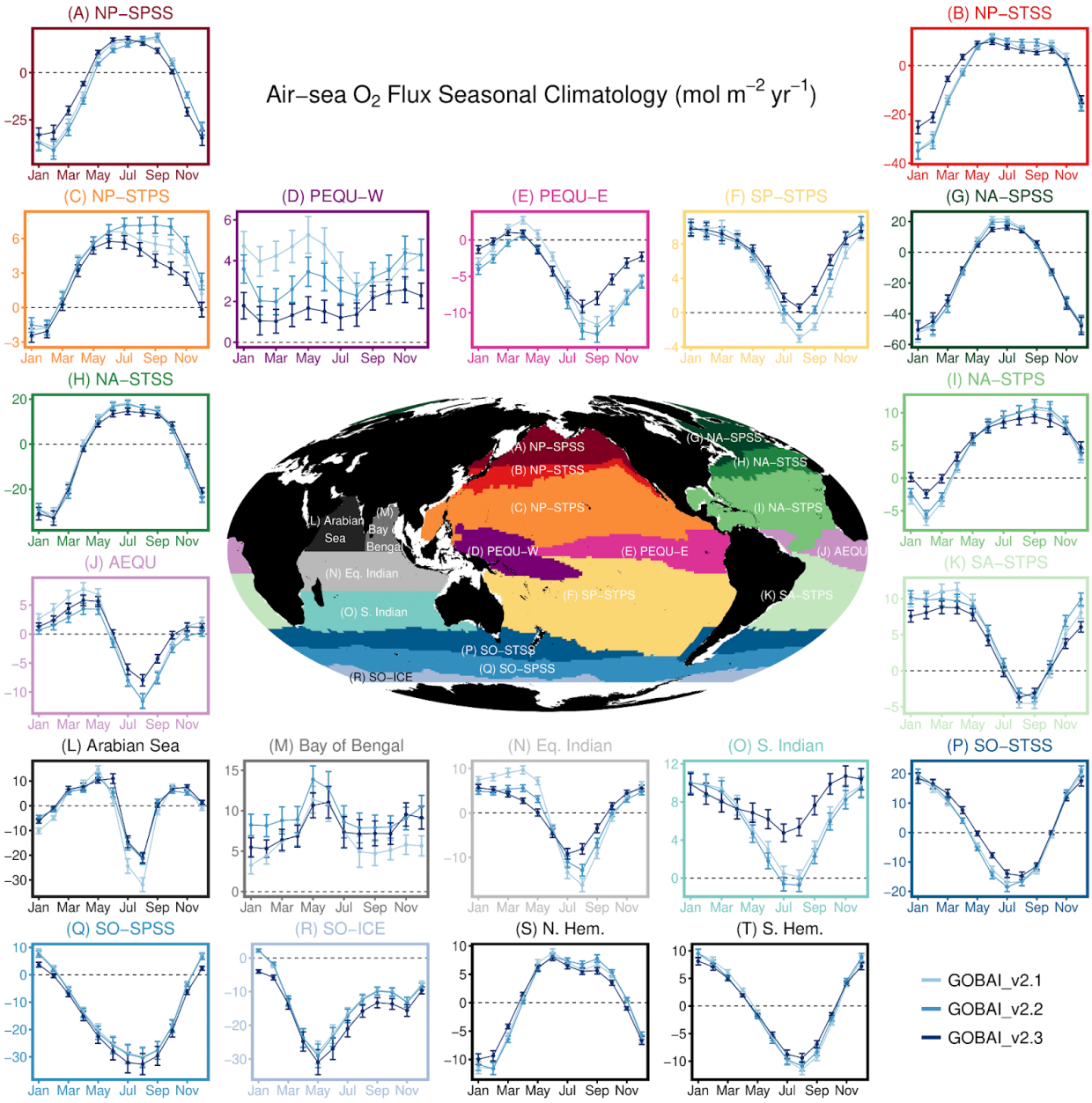

Fig. S4: Similar to Fig. 2, but showing comparison of regional climatological mean seasonal air-sea O_2 flux resolved using DO from three versions of GOBAI-O_2 (by color).

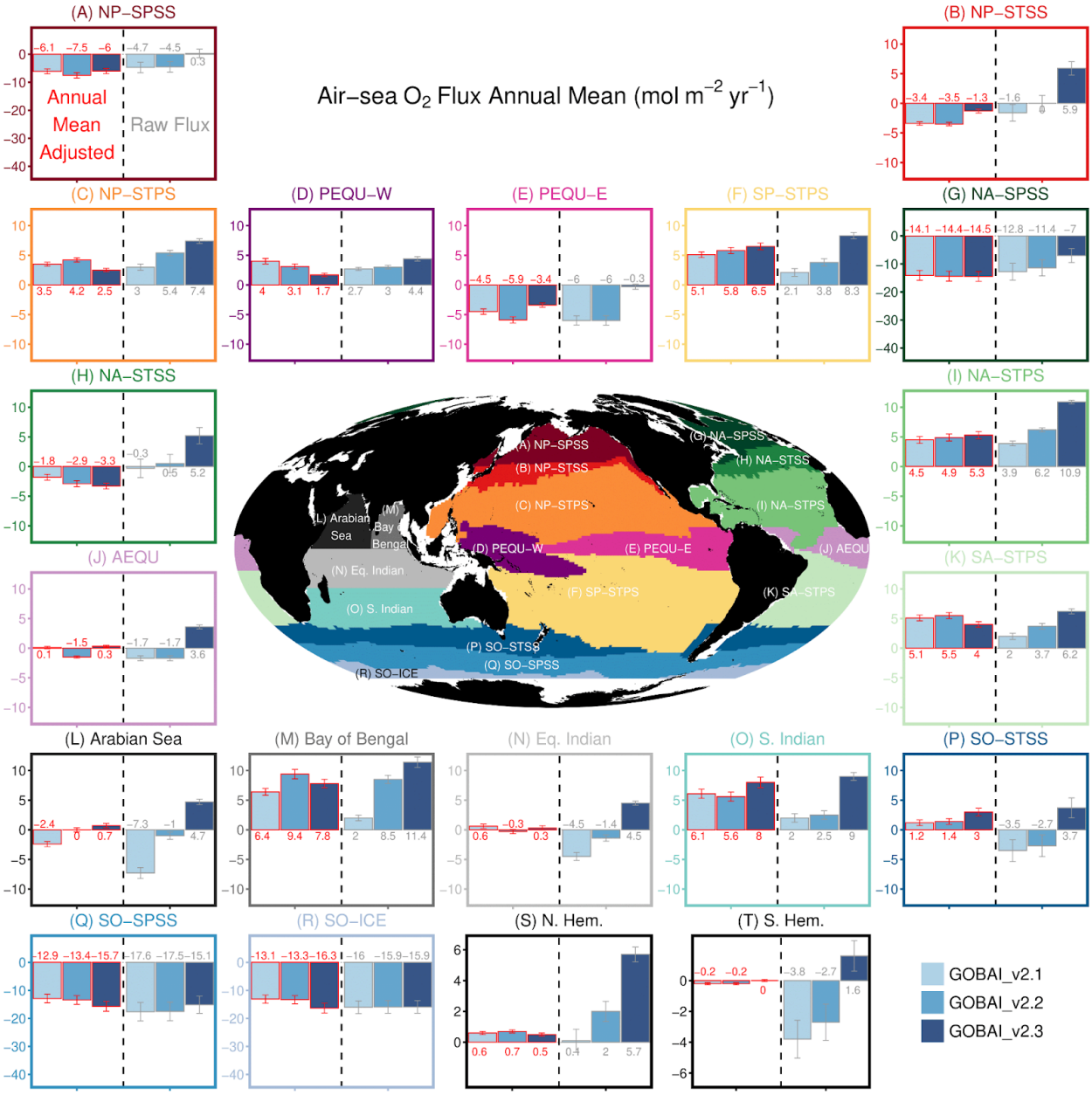

Fig. S5: Similar to Fig. 3, but showing comparison of regional annual mean air-sea O_2 flux resolved using DO from three versions of GOBAI-O_2 (by color).

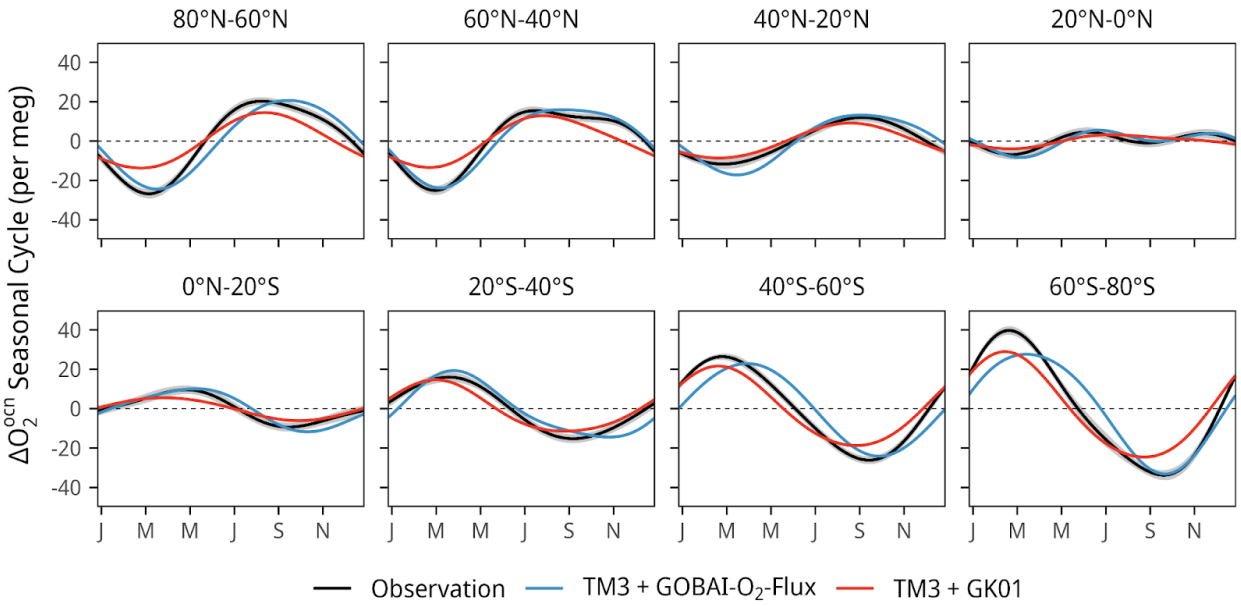

Fig. S6: Similar to Fig. 6, but comparing TM3 simulations of airborne tropospheric-average ΔO_2^{ocn} seasonal cycles using air-sea O_2 flux from GK01 (red, Garcia and Keeling, 2001) and our flux product (blue). The observed ΔO_2^{ocn} seasonal cycles are also shown in black.

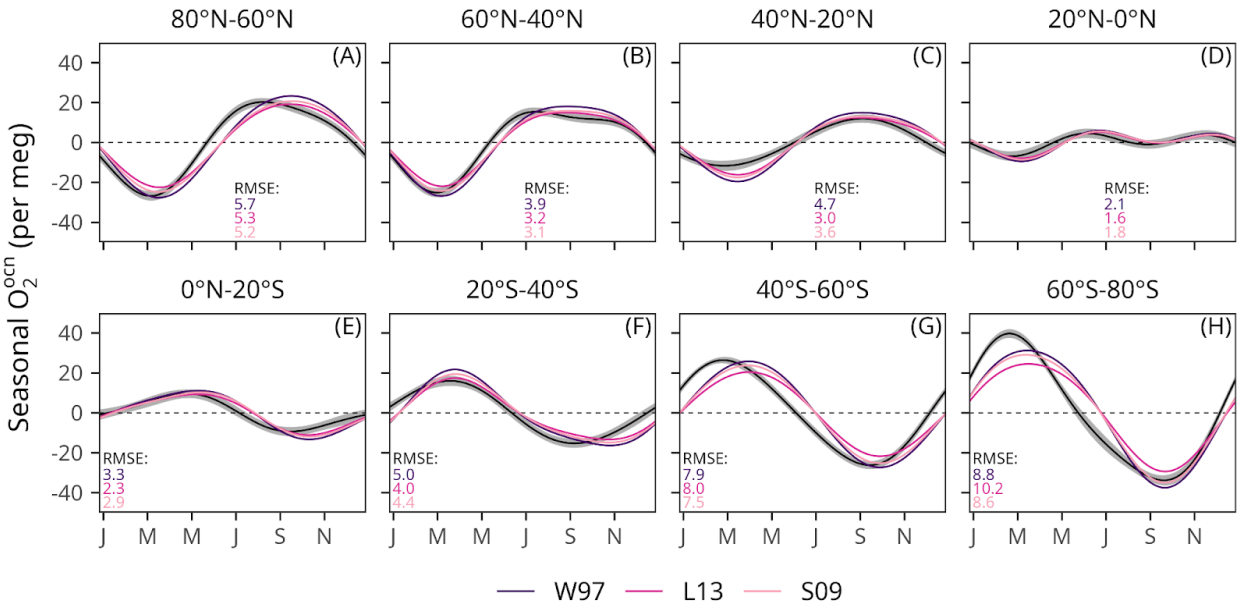

Fig. S7: Similar to Fig. 6, but comparing TM3 + GOBAI-O_2-Flux simulations of airborne tropospheric-average seasonal ΔO_2^{ocn} variations across eight latitude bands computed using different gas exchange parameterization schemes. The simulations are based on TM3 forward transport of ensemble mean fluxes calculated using each of the gas exchange schemes, and CCMP wind products.

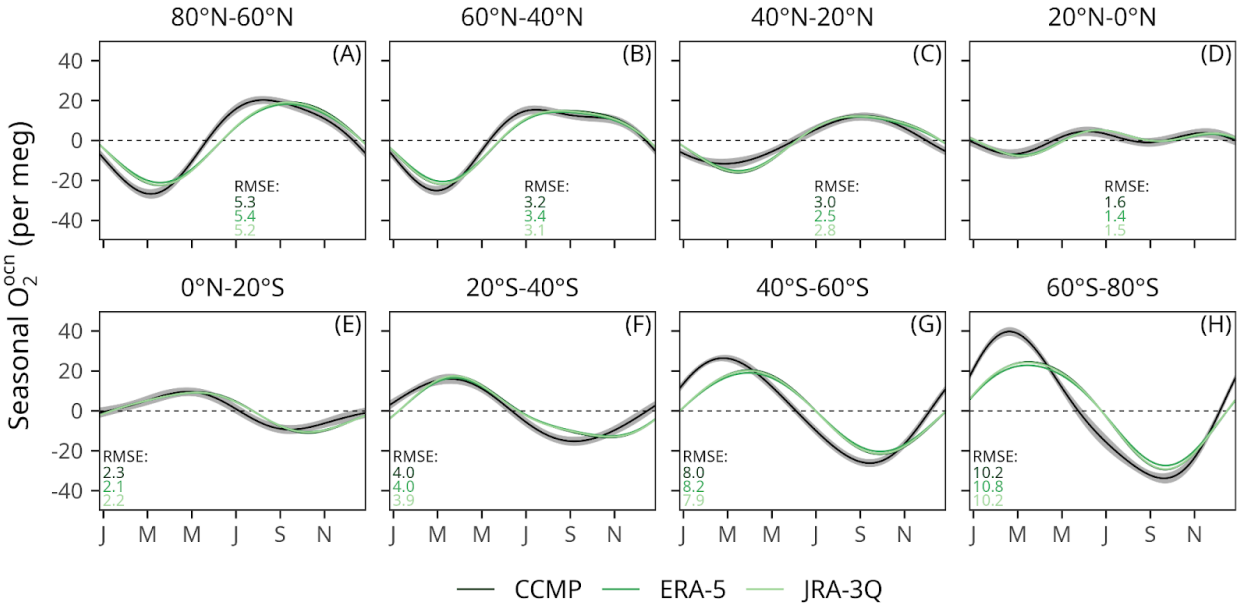

Fig. S8: Similar to Fig. 6, but comparing TM3 + GOBAI-O_2-Flux simulations of airborne tropospheric-average seasonal ΔO_2^{ocn} variations across eight latitude bands computed using different wind products. The simulations are based on TM3 forward transport of ensemble mean fluxes calculated using each of the wind products, and L13 gas exchange parameterization scheme.

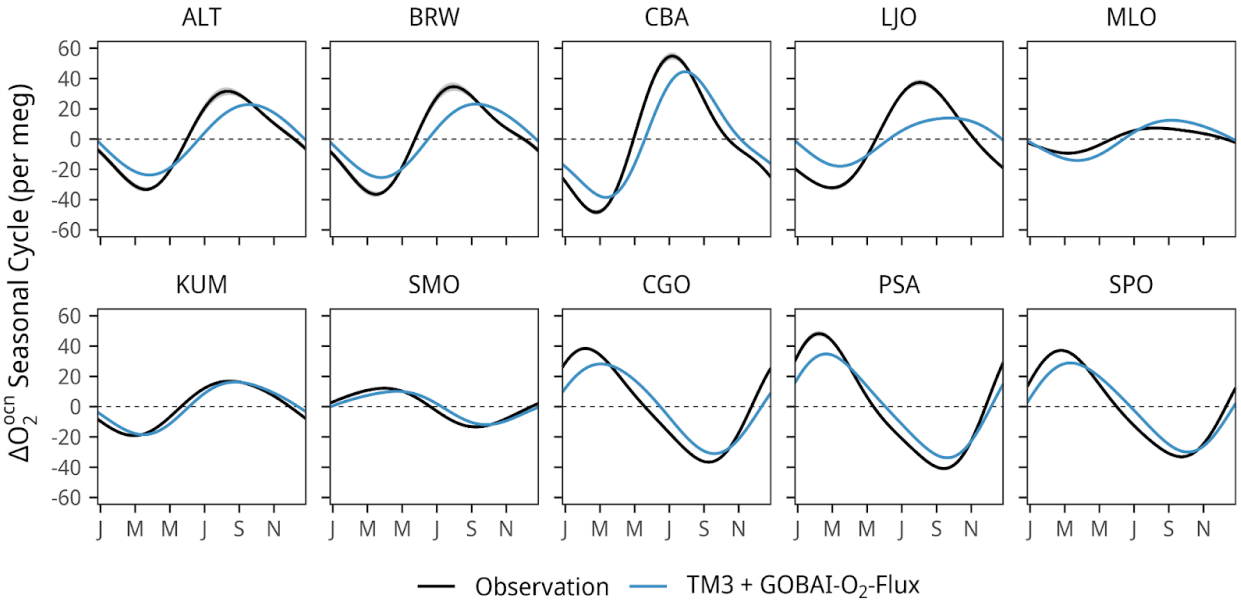

Fig. S9: Comparison of seasonal atmospheric ΔO_2^{ocn} between observations and TM3 + GOBAI-O_2-Flux simulations at 10 surface sampling sites along the Pacific basin. Panels are organized from southernmost to northernmost stations. Seasonal cycles are calculated following the same procedure as in Fig. 6 and averaged over 2005-2020, except for BRW, which is averaged over 2011-2020. Gray shading represents uncertainty of the observed seasonal cycle, combining measurement uncertainty and uncertainty in the atmospheric non-oceanic O_2 component corrections estimated from the ensemble of flux products and transport models (Appendix C).

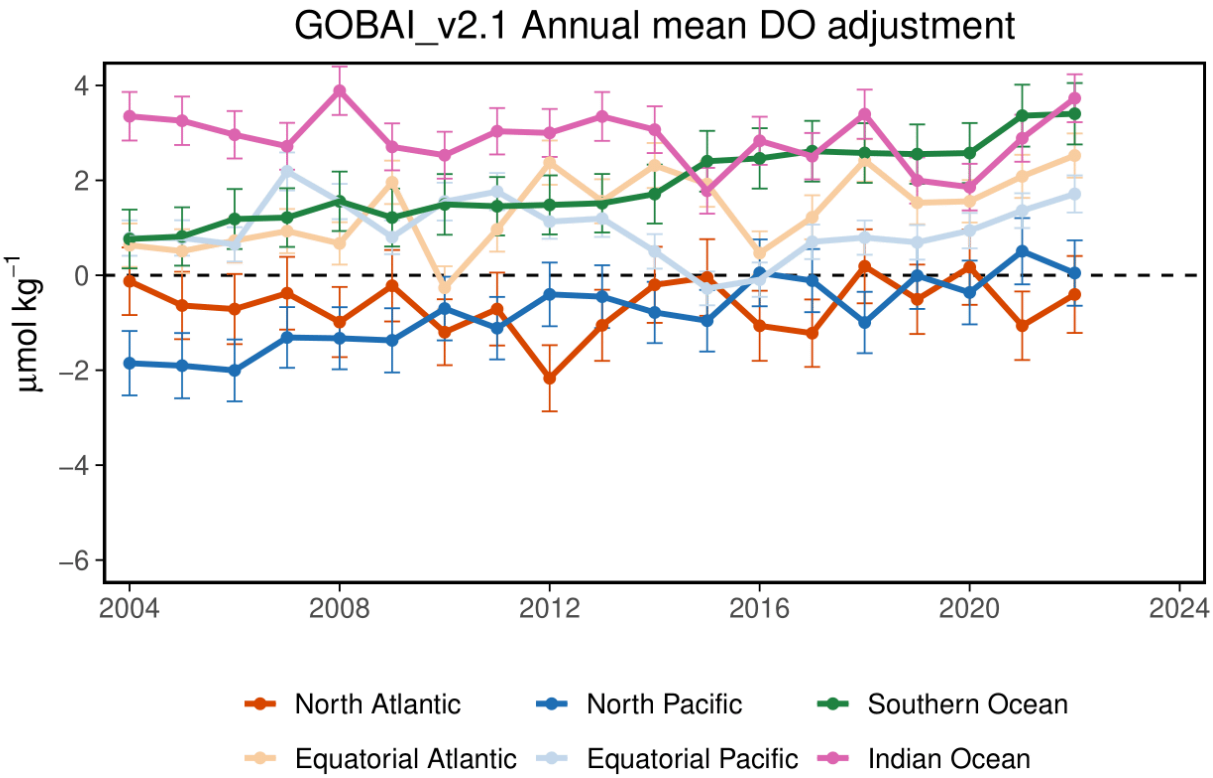

Fig. S10: Similar to Fig. B2, but showing DO adjustment for each of the six ocean regions (in Fig. B1), and each year for GOBAI-O_2 v2.1.

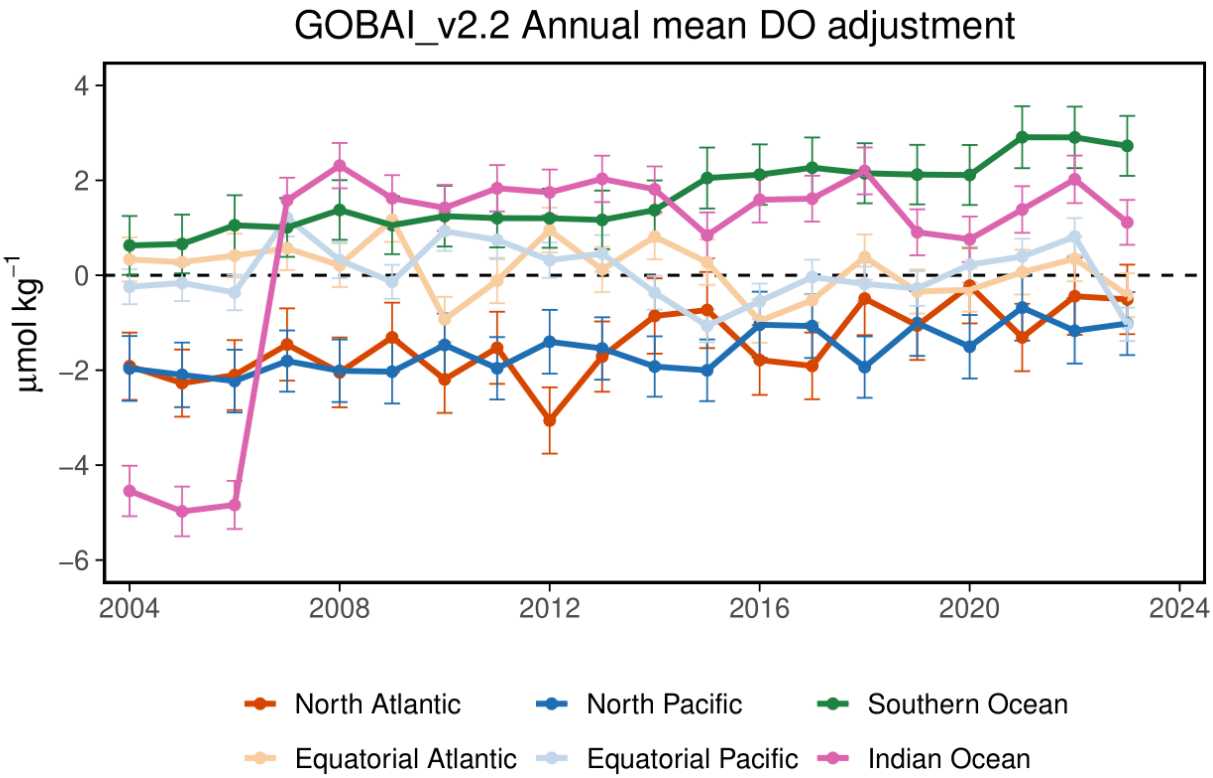

Fig. S11: Similar to Fig. B2, but showing DO adjustment for each of the six ocean regions (in Fig. B1), and each year for GOBAI-O_2 v2.2.

References

Garcia, H. E. and Keeling, R. F.: On the global oxygen anomaly and air-sea flux, J. Geophys. Res. Oceans, 106, 31155–31166, https://doi.org/10.1029/1999JC000200, 2001.